Journal of Alloys and Compounds 517 (2012) 132–138

Contents lists available at SciVerse ScienceDirect

Journal of Alloys and Compounds

journal homepage: www.elsevier.com/locate/jallcom

Surface waves investigation in NiFe/Au/Co/Au multilayers by high-resolution Brillouin spectroscopy

A. Trzaskowska[a,*], S. Mielcarek[a], B. Graczykowski[a], F. Stobiecki[b]

[a] Faculty of Physics, Adam Mickiewicz University, Umultowska 85, 61-614 Poznan, Poland
[b] Institute of Molecular Physics, Polish Academy of Sciences, Smoluchowskiego 17, 60-179 Poznan, Poland

ARTICLE INFO

Article history:
Received 7 October 2011
Received in revised form
12 December 2011
Accepted 14 December 2011
Available online 23 December 2011

Keywords:
Magnetic films and multilayers
Surface phonons
Brillouin scattering spectroscopy

ABSTRACT

The behaviour of Rayleigh and Sezawa surface phonons propagating in magnetic multilayers $[Ni_{80}Fe_{20}/Au/Co/Au]_{10}$ on silicon substrate was studied by high-resolution Brillouin spectroscopy. The dispersion dependence of the phase velocity was determined as a function of wavenumber and the angular dispersion was tested. A simulation of the dispersion dependence was made by the finite element method and the results were compared with those of the experiment.

1. Introduction

Free-standing thin films are the fundamental elements for construction of blocks of microsystems. In the present technology of microsystems production, silicon is the most often used material. A rapid increase in the memory operation frequency in modern computers and applications of ferromagnetic films to the microwave devices motivated special interest in their high-frequency dynamics [1,2]. Nowadays much attention is paid to thin multilayers deposited on silicon substrate [3–5]. From the application viewpoint, the knowledge of elastic properties of nanometric materials is of particular importance. The behaviour of acoustic waves can be investigated by laser acoustics [6] and Brillouin spectroscopy [7]. Brillouin light scattering (BLS) spectroscopy has proved to be one of the most powerful methods providing access to the parameters which monitor the physical properties of nanometric films. This method is based on the inelastic light scattering on the acoustic waves propagating in the medium studied is practically non-destructive one [8,9]. Brillouin spectroscopy is the only technique to study the surface wave dynamics, pseudo-surface waves and bulk waves (longitudinal and transverse) propagating in the medium studied in the range of GHz. Literature provides information only about the elastic properties in the GHz range for bilayers systems of the structure type bcc–fcc, bcc–bcc or fcc–fcc such as Au/Cr, Ni/Mo, Co/Cu or $Ni_{80}Fe_{20}$/Al [10–13].

Results presented in this paper refer to $[Ni_{80}Fe_{20}/Au/Co/Au]_N$ multilayers ($N = 10$; N is the number of repetitions). Structures of this type are particularly interesting because of their possible application in recording media [14] or magnetoresistive sensors [15]. It has been hitherto demonstrated that $[Ni_{80}Fe_{20}/Au/Co/Au]_N$ multilayers display gigantic magnetoresistance and that their magnetic and magnetoresistive properties can be modified in a broad range by adjusting layers thickness [16] and/or by using composite magnetic layers [17]. The question is what is the behaviour of surface acoustic waves upon modification of the cobalt layer thickness.

The main aim of the study was to determine the dispersion dependencies of the phase velocities of Rayleigh and Sezawa waves as a function of the wavenumber of $[Ni_{80}Fe_{20}/Au/Co/Au]_{10}$ deposited on silicon substrate. Moreover, anisotropy of the phase frequency of surface acoustic waves (SAW) was evaluated in the propagation direction in the plane (1 1 1) in the multilayers studied. Measurements were performed by the high-resolution Brillouin light scattering spectroscopy. The behaviour of surface Rayleigh waves and Sezawa waves propagating in the multilayer systems studied was analysed. Using the finite element method (FEM) [18,19] a simulation of propagation of the surface waves in the multilayer structures was made. The experimental results were compared with those obtained by FEM simulation.

2. Experimental

The $[Ni_{80}Fe_{20}/Au/Co/Au]_N$ multilayers ($N = 10$, number of repetition) studied were deposited in Ar atmosphere using high vacuum magnetron sputtering on Si (1 0 0) naturally oxidized substrate. For details check Ref. [20]. The thickness of $Ni_{80}Fe_{20}$ and Au layers was 2 nm, while that of the cobalt layer was different in

* Corresponding author. Tel.: +48 61 8295190.
E-mail address: olatrzas@amu.edu.pl (A. Trzaskowska).

0925-8388/$ – see front matter © 2011 Elsevier B.V. All rights reserved.
doi:10.1016/j.jallcom.2011.12.059

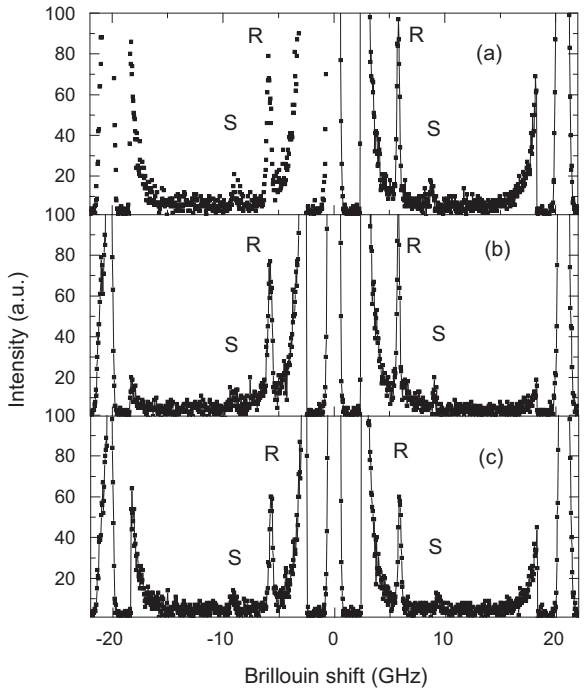

Fig. 1. Exemplary Brillouin SAW spectra of $[Ni_{80}Fe_{20}/Au/Co/Au]_{10}$ multilayer with the cobalt layer thickness of 0.4 nm (a), 0.8 nm (b) and 1.2 nm (c).

particular samples and equal to 0.4 nm, 0.8 nm or 1.2 nm. The sputtering rates were 0.06, 0.05, and 0.045 nm/s, for Au, $Ni_{80}Fe_{20}$ and Co, respectively.

The sandwich structures were investigated using high resolution Brillouin light scattering. The BLS measurement were made in the backscattering geometry. Light from a single mode Nd:YAG laser of wavelength $\lambda = 532$ nm was focused onto the sample surface. The backscattering light was collected by using *f*/8 optics, focal length 58 mm. The solid angle of the lens was 0.63 steradians. Inelastic scattered light was analysed using Sandercock – type 3 + 3 pass tandem Fabry–Perot interferometer. A detailed description of the spectrometer has been given elsewhere [21]. The value of the wavevector was changed by varying the angle of the light incidence Θ measured against the surface normal of the sample: $k = (4\pi/\lambda)\sin\Theta$ in the range $2.21 \times 10^7\ m^{-1}$ to $0.53 \times 10^7\ m^{-1}$. In order to get the best BLS spectrum of phonons propagating in the multilayers studied, the polarization of the incident and scattered light was parallel to the sagittal plane defined by the wavevector of a given phonon and the normal to the sample surface [22].

3. Results

For opaque materials the light is scattered on the surface of the material according to the surface ripple mechanism [23,24], while for transparent materials the light is scattered mainly in the bulk of the sample according to the photoelastic coupling mechanism [8,25]. The light penetration depth of multilayer systems studied are about few nanometers. Exemplary Brillouin spectra of the samples studied, collected for $\Theta = 45^\circ$ are shown in Fig. 1.

For all samples studied the spectra show surface Rayleigh modes (*R*) and Sezawa modes (*S*) of the first order. The higher order Sezawa modes were characterised by low intensity. Modes identification is based on further FEM calculation.

The phase velocities of propagation of the surface modes were determined on the basis of the relation:

$$\Delta\nu = \frac{2\sin\Theta}{\lambda}\upsilon \quad (1)$$

where: $\Delta\nu$ – Brillouin frequency shift of each peak, Θ – the angle made by the incident beam to the normal to the surface, λ – the laser wavelength, υ – velocity of surface mode propagation. Results are given in Table 1.

According to the results, with increasing thickness of the cobalt layer (t_{Co}) the velocity of Rayleigh surface wave decreases, although the change is very small. In contrast, the Sezawa wave velocity increases with increasing cobalt layer thickness. Measurements of SAW propagation velocity performed in the whole accessible range of wavevector permitted drawing the dispersion dependence $\upsilon(kh)$.

Table 1
Velocity of surface modes propagation in the multilayers studied.

	υ_R Rayleigh mode (m/s)	υ_S Sezawa mode (m/s)
$[Ni_{80}Fe_{20}/Au/Co/Au]_{10}$ $t_{Co} = 0.4$ nm	1980 ± 20	3170 ± 30
$[Ni_{80}Fe_{20}/Au/Co/Au]_{10}$ $t_{Co} = 0.8$ nm	1960 ± 20	3260 ± 30
$[Ni_{80}Fe_{20}/Au/Co/Au]_{10}$ $t_{Co} = 1.2$ nm	1950 ± 20	3380 ± 30

Phase velocity υ dispersion curves for the discrete sagittally polarized surface waves Rayleigh and Sezawa waves as a function of *kh* are presented in Fig. 2. As the materials studied make a 10 times repeated multilayer system, the thickness *h* of the multilayers system was assumed $h = 10 \times (2 \times t_{Au} + t_{Ni_{80}Fe_{20}} + t_{Co})$ where t_{Au} – thickness of the gold layer, $t_{Ni_{80}Fe_{20}}$ – thickness of the permalloy layer.

As follows from the character of the dispersion dependence, the materials studied can be classified as the slow-on-fast systems [26,27]. The dispersion curve for the slow-on-fast system for a Rayleigh mode has a negative slope and begins at $kh = 0$ with the Rayleigh wave velocity characteristic of the substrate and should asymptotically decrease to the value typical of a layer of uniform material deposited on the substrate [26,27]. The surface Rayleigh wave velocity in the multilayers studied for $kh = 0$ is typical of silicon substrate (1 0 0) $\upsilon_R^{substrate} = 4910$ m/s [26], see Fig. 2. As the samples studied were multiple layers of $[Ni_{80}Fe_{20}/Au/Co/Au]_{10}$ supported on Si (1 0 0) naturally oxidized, the dispersion dependence for large *kh* does not reach the values of Rayleigh surface phonon velocity υ_R^{film} characteristic of each of the uniform one-component layers (Au, Co, $Ni_{80}Fe_{20}$). The velocities of the surface Rayleigh wave for high *kh* were determined by the FEM method, described in Section 5. The dispersion dependence is a decreasing exponential function; at $kh \to 0$ it is difficult to establish the initial velocity. The fitting procedure of the Sezawa wave dispersion dependence presented in Fig. 2 refers to the multilayer in which the thickness of a single sandwich is 6.4 nm, 6.8 nm and 7.2 mn.

The angular dispersions of the modes observed were also determined, the results are presented in Fig. 3. The mode frequency dependencies on the propagation direction in the planes studied were collected for $\Theta = 45^\circ$.

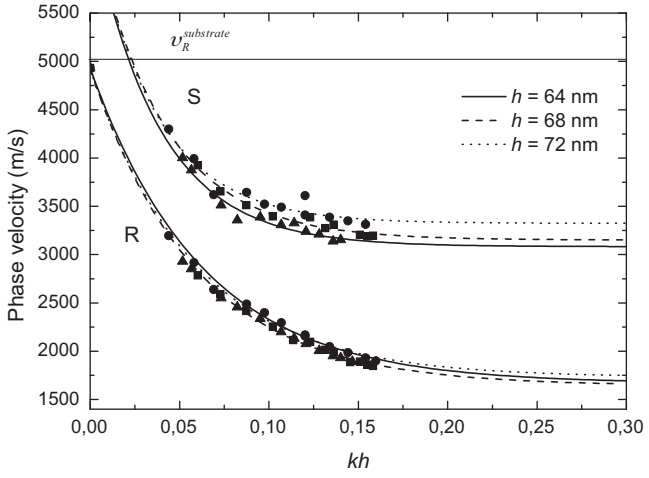

Fig. 2. Dispersion relations for the SAW propagating in the multilayer systems of the thicknesses *h*: (●) *h* = 72 nm, (■) *h* = 68 nm, (▲) *h* = 64 nm. The lines are the exponential fit to the measuring points.

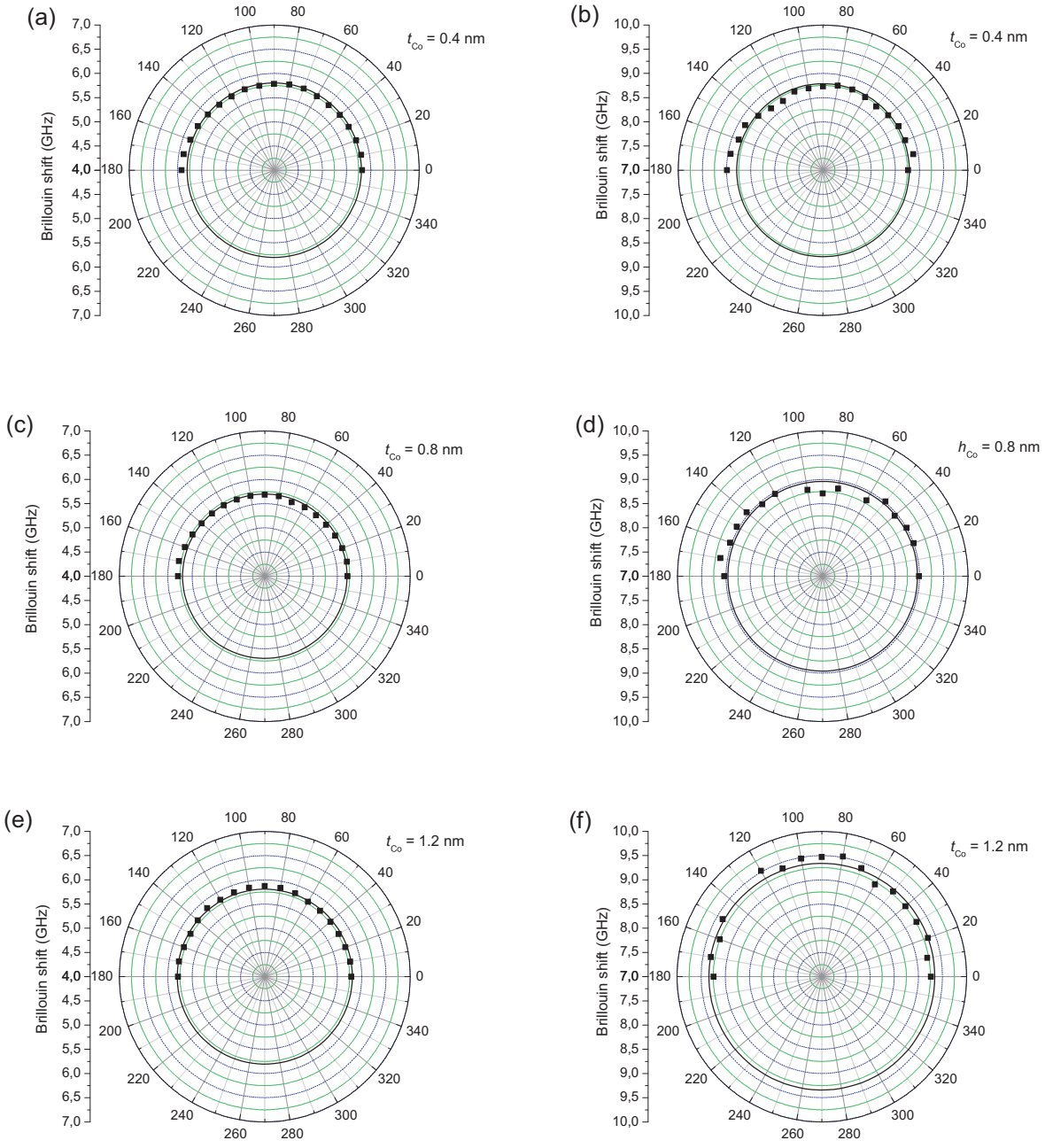

Fig. 3. Angular dispersion of SAW for the samples studied containing cobalt layers of different thicknesses t_{Co} (a, c, and e) Rayleigh wave, (b, d, and f) Sezawa wave; (1 0 0) oriented substrate and (1 1 1) oriented sandwiches.

For individual samples, the frequency anisotropy of the modes studied did not change; the angular dispersion of the mode frequency was isotropic both for the surface Rayleigh and Sezawa waves. The modes' velocities were independent of propagation direction in the studied plane.

4. FEM simulations

In order to establish theoretically the dispersion dependence for the modes propagating in the structures studied, a simulation study was performed by the FEM in which only the unit cell is meshed. Schematic presentation of the multilayer structure made of $[Ni_{80}Fe_{20}/Au/Co/Au]_{10}$ supported on a semi-infinite silicon substrate is shown in Fig. 4.

The substrate is treated as a cubic uniform elastic half-space $z \leq 0$. It supports a multilayered system of exactly determined thicknesses of each layer. The model assumes perfectly bonded, ideally flat parallel layers with zero interfacial thickness and uniform respective layer thickness, no roughness and defects, with constant elastic properties within a given layer. The elastic constants and the densities of each sandwich studied are given in Table 2. To take into account the orientations of the sandwiches with respect to the (1 1 1) plane, the main components of the elasticity tensor were rotated accordingly. To calculate the dispersion diagrams in this study we used COMSOL MULTIPHYSICS [28].

In order to reflect the conditions of the elastic semispace, the specific boundary conditions were adapted for the elementary cell shown in Fig. 4. For the walls perpendicular to the free surface the

Table 2
Physical characterisation of the materials used; ρ – density (kg/m^3), c_{ij} – main components of the elasticity tensor ($\times 10^{10}$ N/m^2).

Constant	Silicon (Si) [29]	Permalloy ($Ni_{80}Fe_{20}$) [30]	Gold (Au) [31]	Cobalt (Co) [32]
ρ	2331	8690	19,300	8836
$c_{11} = c_{22}$	16. 6	2.5	1.923	3.071
c_{33}	16. 6	2.5	1.923	3.581
$c_{44} = c_{55}$	7.96	0.63	0.419	0.755
c_{66}	7.96	0.63	0.419	0.710
c_{12}	6.4	2.185	1.631	1.65
$c_{13} = c_{23}$	6.4	2.185	1.631	1.027

Bloch–Floquet periodic boundary conditions were applied for each of the three components of displacement [33]:

$$\begin{aligned} &u\ \exp[i(k_x x + k_y y + k_z z)],\\ &v\ \exp[i(k_x x + k_y y + k_z z)],\\ &w\ \exp[i(k_x x + k_y y + k_z z)], \end{aligned} \tag{2}$$

where u, v, w denote the components of displacement in a rectangular coordinate system, while the wavevector components can be written:

$$\begin{aligned} k_x &= k\ \cos\ \alpha = \frac{2\pi\ \cos\ \alpha}{\lambda_{SAW}},\\ k_y &= k\ \cos\ \beta = \frac{2\pi\ \cos\ \beta}{\lambda_{SAW}},\\ k_z &= k\ \cos\ \gamma = \frac{2\pi\ \cos\ \gamma}{\lambda_{SAW}}, \end{aligned} \tag{3}$$

In these expressions angles α, β, γ denotes the angles between the wavevector and axes x, y, z of the coordinate system respectively, λ_{SAW} is the wavelength of SAW.

The exponential decay of the SAW amplitude was taken into regard by the free boundary condition for the free surface and a fixed boundary condition ($u = v = w = 0$) for the opposite wall.

In this case assume that the wavevector component k_z is zero (wavevector of surface wave lies in the plane xy) so:

$$\cos\ \beta = \cos(90 - \alpha) = \sin\ \alpha \tag{4}$$

Based on the expressions of solid state mechanics it is possible to determine free energies of the deformed body on unit volume:

$$F = \frac{1}{2} c_{ijkl} u_{ij} u_{kl}, \tag{5}$$

where: c_{ijkl} is the elasticity tensor, u_{ij} is the deformation tensor (small deformation): $u_{ij} = (\partial u_i/\partial x_j + \partial u_j/\partial x_i)/2$. In this case: $(u_1, u_2, u_3) = (u, v, w)$.

The criterion of the search for surface waves is the relative position of the free energy density centre along the axis z. An exemplary solution showing the relative displacement field and arrows correspond to the relative deformation for a Rayleigh surface wave and Sezawa wave, is shown in Fig. 5.

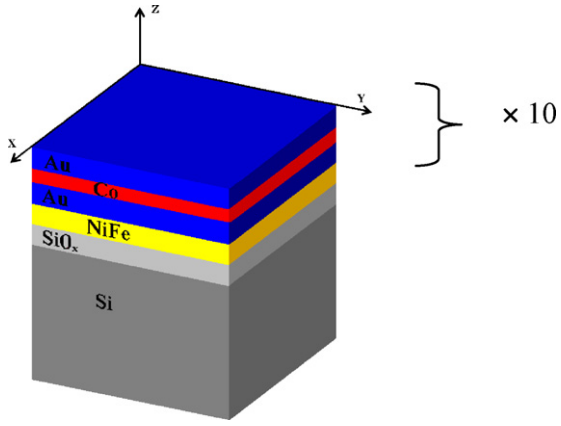

Fig. 4. A scheme of the multilayered structure studied.

Analysis of the total displacement has shown that the penetration depth of the Rayleigh surface wave is twice greater than that of the Sezawa wave, which is in agreement with the Farnell's theory [26]. No essential differences were noted in the SAW penetration depth for the multilayers with cobalt layers of different thicknesses. FEM simulations performed for the multilayers have proved that the cobalt layer thicknesses changes of an order of 0.4 nm do not cause essential changes in the penetration depth of Rayleigh and Sezawa waves in the systems studied.

The dispersion dependencies $\Delta v(k)$ obtained for the multilayer systems studied are shown in Fig. 6.

A very good agreement was obtained between the experimental and theoretical (FEM simulation) dispersion dependencies for Sezawa waves. The poorer agreement obtained for Rayleigh surface waves is a consequence of a curvature in the dispersion dependence for the system made of a uniform layer supported on a semi-infinitive substrate [26]. Moreover, the character of dispersion dependence of a Rayleigh wave significantly depends on the procedure of a sandwich system preparation. Subsequent layers do not have atomic-smooth surfaces and in the interface the neighbouring layers can partly penetrate each other [14–17], while the simulations assume perfectly bonded and ideally flat parallel layers.

5. Discussion

In order to determine the actual effect of the cobalt layer thicknesses on the velocity of surface wave propagation in the materials studied, a simulation of SAW propagation was made by FEM for the multilayered systems with the cobalt layers of different thicknesses. The results obtained for the wavevector of $k = 0.88 \times 10^7$ m^{-1} are presented in Fig. 7.

Changes in the cobalt layer thickness have little influence on the frequency of Rayleigh surface waves, but cause significant changes in the Sezawa waves. In the multilayered systems studied the number of sandwiches N in the multilayered systems has the greatest influence on the surface waves propagation, which is illustrated in Fig. 8. When the number of sandwiches exceeds 15 so the samples could be treated as multilayers materials with $N > 15$, the Rayleigh and Sezawa wave propagation velocities would reach minima of 1700 m/s and 3000 m/s, respectively.

Taking into account that the amplitude of the surface waves diminishes with the depth of the wave penetration, the waves propagate on great distances in the silicon substrate. In view of the small thickness of the sandwiches in comparison to the length of the surface waves, in the wavevector range studied the wavelength varies from ~280 nm to ~1500 nm, the question arises if the multilayered system can be treated as a uniform material. To answer this question it was necessary to determine the mean density and components of the elasticity tensor of the whole system of multilayers assuming that it is a uniform material. Determination of individual elastic components was possible by imposing periodic boundary conditions onto a single sandwich to make an infinite periodic multilayer structure simulating a bulky compound made of an

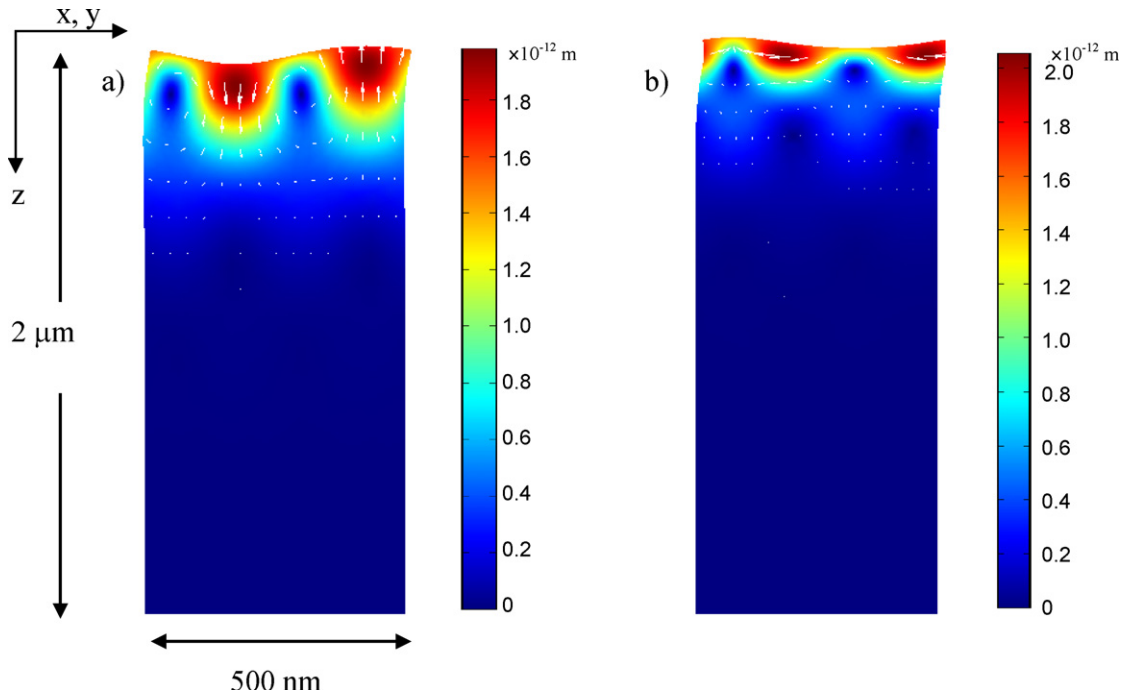

Fig. 5. Relative displacement field with deformed shape for Rayleigh surface wave (a) Sezawa wave (b). The colour legend shows the magnitude of relative displacements. (For interpretation of the references to color in this figure legend, the reader is referred to the web version of the article.)

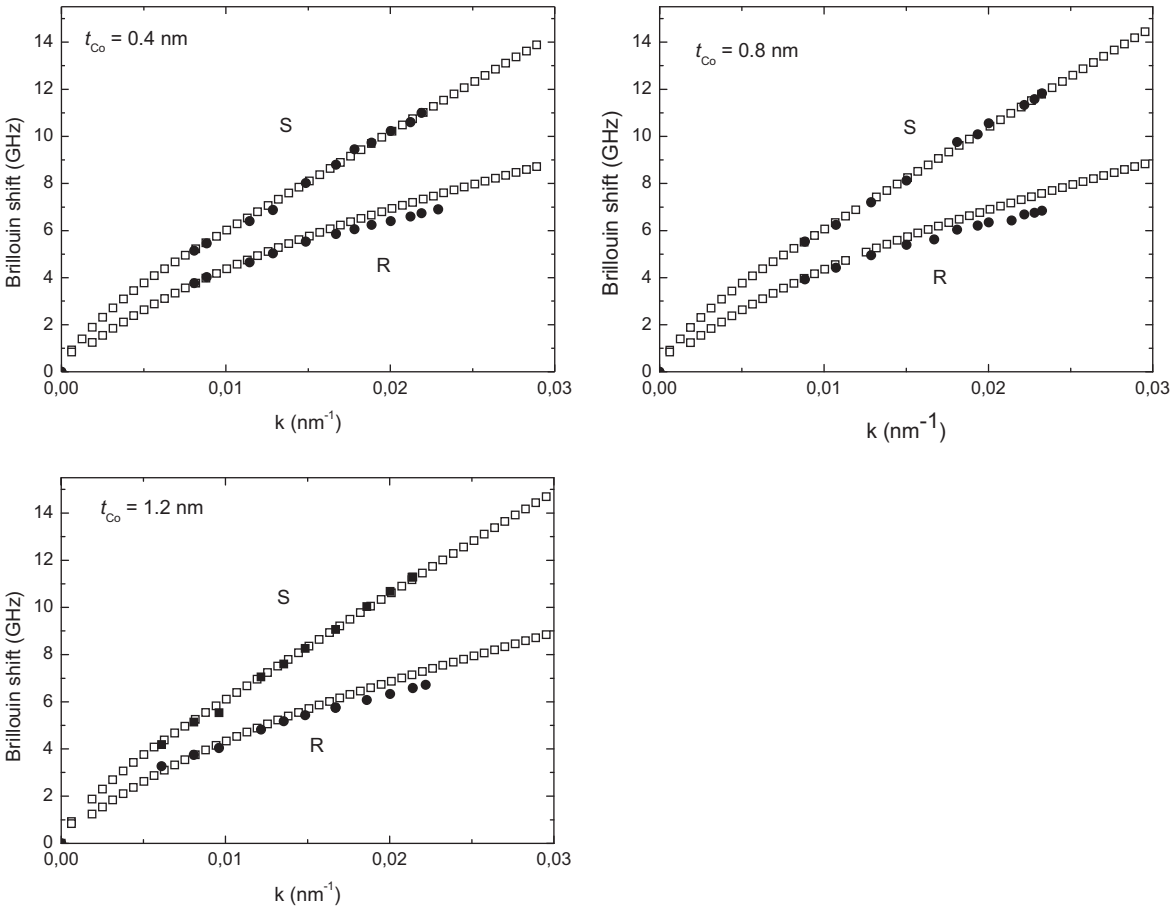

Fig. 6. The dispersion dependence of the Rayleigh surface waves (*R*) and Sezawa waves (*S*) calculated by the FEM method (□) with the experimental results (●) for the multilayered systems with Co layer of different thicknesses t_{Co}.

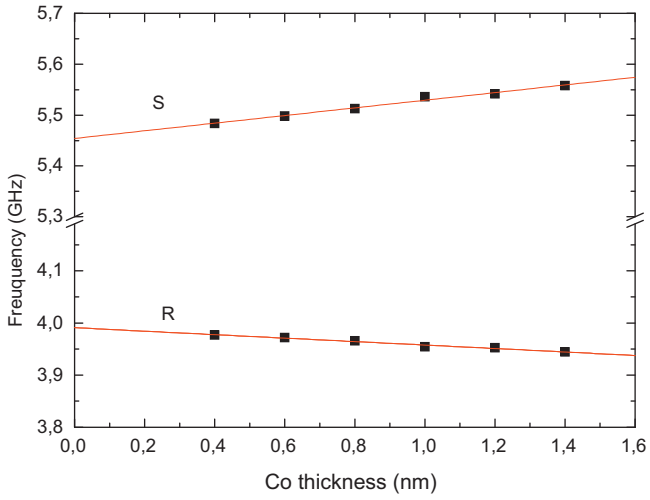

Fig. 7. Calculated changes in the frequencies of surface waves propagation versus the thickness of the cobalt layer in the multilayered system.

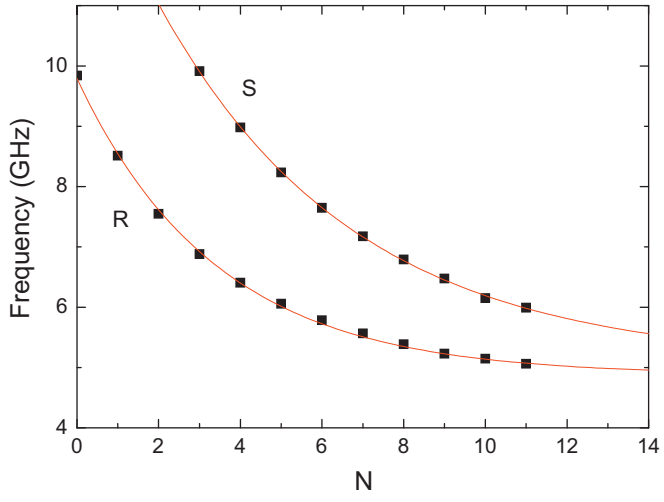

Fig. 8. Calculated changes in the frequency of surface wave propagation in response to the number N of the $Ni_{80}Fe_{20}$/Au/Co/Au sandwiches deposited on silicon substrate.

infinite number of sandwiches. In the wavevector range studied such an approach permitted calculation of the propagation velocities of longitudinal and transverse waves in thus defined material, which permitted determination of the elasticity tensor components, see Table 3. The waves propagate in the direction parallel to the interface planes.

For a system made of a uniform layer of the above parameters deposited on a (1 0 0) silicon substrate a simulation was performed by FEM in order to determine a dispersion dependence. Fig. 9 shows the results calculated for the uniform bulk approximation (squares), for the multilayered structure (triangle) and the

Table 3
Calculated components of the elasticity tensor c_{ij} ($\times 10^{10}$ N/m^2) and density ρ (kg/m^3) of the samples made of an infinite number of sandwiches versus the thickness t (nm) of the cobalt layer.

Constant	t_{Co} = 0.4	t_{Co} = 0.8	t_{Co} = 1.2
ρ	15,330	14,948	14,608
$c_{11} = c_{22} = c_{33}$	20.53	21.36	21.54
$c_{44} = c_{55} = c_{66}$	4.28	4.47	4.55
$c_{13} = c_{23} = c_{12}$	11.99	12.41	12.43

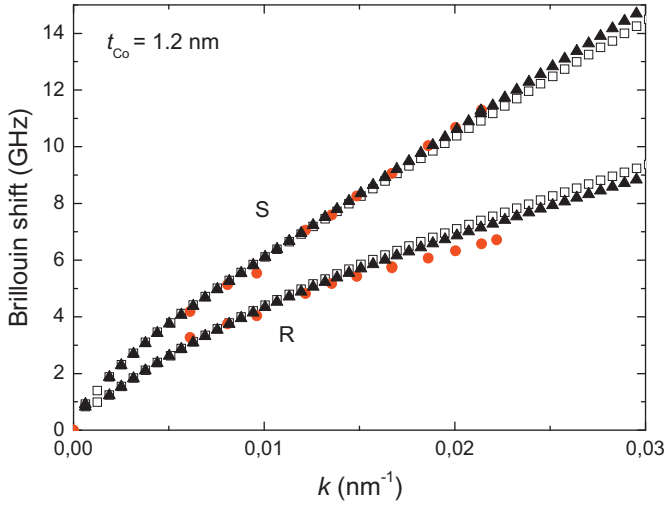

Fig. 9. Dispersion dependencies obtained by FEM for (□) uniform material simulating a series of sandwiches, (▲) a series of sandwiches with the cobalt layer thickness of t_{Co} = 1.2 nm on the silicon substrate and (●) the experimental data points.

Table 4
Velocities of the Rayleigh surface wave (m/s) determined for the uniform material simulating a series of sandwiches with the cobalt layer thickness of t_{Co} (nm).

Constant	t_{Co} = 0.4	t_{Co} = 0.8	t_{Co} = 1.2
υ_R^{film}	1570	1620	1650

experimental data points (circles) obtained for the real sample with the cobalt layer thickness of 1.2 nm.

The results obtained assuming the uniform bulk approximation (□) are in a very good agreement with those obtained from simulations for a series of sandwiches (▲). The differences in the dependencies obtained by simulations appear for large wavevector values k, outside the range accessible in Brillouin spectroscopy.

Under the assumption that a series of sandwiches can be treated as a uniform material in a certain wavevector range it was possible to determine the velocity of the surface Rayleigh wave, typical of a uniform material without support (υ_R^{film}), Table 4.

The propagation velocities of Rayleigh surface and transverse waves calculated for the uniform bulk material permitted determination of the Rayleigh surface wave velocity. The experimental

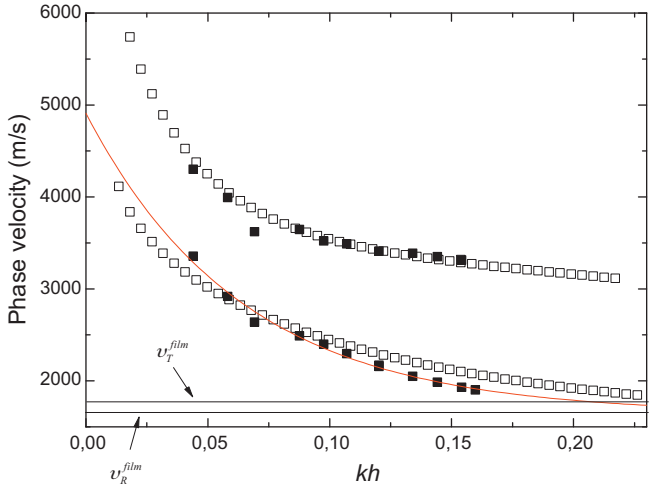

Fig. 10. Dispersion dependencies (□) obtained by FEM simulation and (■) experimentally measured for a series of sandwiches with the cobalt layer thickness of t_{Co} = 1.2 nm. The line is the exponential fit to the measuring points.

SAW dispersion dependence, shown in Fig. 2, is of the slow-on-fast type [26,27]. For the materials showing the dispersion dependence of this type, the Rayleigh surface wave velocity for high *kh* should tend to the values from the Rayleigh wave velocity for a film υ_R^{film} to the velocity of the slowest transverse mode υ_T^{film} in a given film [26,27], Fig. 10.

As shown in Fig. 10, the Rayleigh surface wave velocities in the series of sandwiches on silicon substrate for high *kh* are in the range $\upsilon_R^{\text{film}} < \upsilon_R < \upsilon_T^{\text{film}}$, which is an additional confirmation of the type of the dispersion dependence.

6. Conclusions

The paper presents the dispersion dependence and angular dispersion of Rayleigh and Sezawa waves in multilayered systems made of $[Ni_{80}Fe_{20}/Au/Co/Au]_{10}$ sandwiches of different thicknesses of Co layer supported on silicon substrate, determined by the Brillouin spectroscopy. It has been established that changes in the Co layer thickness in the systems studied have insignificant effect on the propagation velocity of the Rayleigh surface waves but significantly affects the propagation velocity of the Sezawa waves. The dispersion relation obtained is of the slow-on-fast type. Experimental results have been compared with those of a simulation of SAW dispersion relation by FEM. Comparative analysis of the experimental and simulated results has indicated that the multilayered system can be approximated as a uniform material characterised by the parameters given in Tables 3 and 4. Assuming this approximation it has been possible to establish the limiting values of the Rayleigh surface wave velocities to which tends the dispersion relation experimentally found.

Acknowledgment

This work has been partially supported by Grant no. N202 230637 from the Polish Ministry of Science and Higher Education.

References

[1] J.-G. Zhu, Y. Design, in: B. Hillebrands, K. Ounadjela (Eds.), Spindynamics in Confined Magnetic Structures, Topics in Applied Physics, vol. 83, Springer, Berlin, 2001, pp. 289–324.
[2] B. Kuanr, Z. Celinski, R.E. Camley, Appl. Phys. Lett. 83 (2003) 3969–3971.
[3] X.M. Cheng, S. Urazhdin, O. Tschernyshyov, C.L. Chien, V.I. Nikitenko, A.J. Shapiro, R.D. Shull, Phys. Rev. Lett. 94 (2005) 017203-1–017203-4.
[4] F.B. Mancoff, J. Hunter Dunn, B.M. Clemens, R.L. White, Appl. Phys. Lett. 77 (2000) 1879–1881.
[5] S. Mangin, D. Ravelosona, J.A. Katine, M.J. Carey, B.D. Terris, E.E. Fullerton, Nat. Mater. 5 (2006) 210–215.
[6] P. Babilotte, P. Ruello, D. Mounier, T. Pezeril, G. Vaudel, M. Edely, J.-M. Breteau, V. Gusev, Phys. Rev. B 81 (2010) 245207-1–245207-14.
[7] J.R. Sandercock, in: M. Cardona, G. Güntherodt (Eds.), Light Scattering in Solids, Topics in Applied Physics, vol. 51, Springer, New York, 1982, pp. 173–206.
[8] A.G. Every, Measur. Sci. Technol. 13 (2002) R21–R39.
[9] H.Z. Cummins, in: H.Z. Cummins, A.P. Levanyuk (Eds.), Light Scattering Near Phase Transitions, North-Holland, Amsterdam, 1983, pp. 359–447.
[10] P. Bisanti, M.B. Borodsky, G.P. Felcher, M. Grimsditch, L.R. Sill, Phys. Rev. B 35 (1987) 7813–7819.
[11] F. Martin, C. Jaouen, J. Pacaud, G. Abadias, Ph. Djemia, F. Ganot, Phys. Rev. B 71 (2005) 045422-1–045422-14.
[12] G. Carlotti, G. Gubbiotti, L. Pareti, G. Socino, G. Turilli, J. Magn. Magn. Mater. 165 (1997) 424–427.
[13] C. Rossignol, B. Perrin, B. Bonelio, P. Djemia, P. Moch, H. Hurdequint, Phys. Rev. 70 (2004) 094102-1–094102-12.
[14] F. Stobiecki, B. Szymański, T. Luciński, J. Dubowik, M. Urbaniak, K. Roll, J. Magn. Magn. Mater. 282 (2004) 32–38.
[15] F. Stobiecki, M. Tekielak, T. Weis, J. Dubowik, M. Urbaniak, B. Szymanski, M. Schmidt, T. Lucinski, A. Ehresmann, A. Maziewski, 19-th International Colloquium on Magnetic Films and Surfaces (ICMFS 2006), Sendai, Japonia, 2006, pp. 14–18.
[16] M. Urbaniak, F. Stobiecki, B. Szymański, M. Koncewicz, J. Phys.: Condens. Matter. 20 (2008) 085208-1–085208-4.
[17] F. Stobiecki, M. Urbaniak, B. Szymański, M. Schmidt, T. Luciński, Phys. Status Solidi B 243 (2006) 210–213.
[18] W.B.J. Zimmerman, Multiphysics Modeling with Finite Element Methods (Series on Stability, Vibration and Control of Systems, Serie), World Scientific Publishing Company, 2006.
[19] W.B.J. Zimmerman, Process Modelling and Simulation with Finite Element Methods (Stability, Vibration and Control of Systems, Series A) by William B.J. Zimmerman, World Scientific Publishing Company, 2004.
[20] M. Urbaniak, F. Stobiecki, B. Szymański, A. Ehresmann, A. Maziewski, M.J. Tekielak, J. Appl. Phys. 101 (2007) 013905-1–013905-7.
[21] J.R. Sandercock, J. Phys. E: Sci. Instrum. 9 (1976) 566–569.
[22] R. Loudon, J.R. Sandercock, J. Phys. C: Solid State Phys. 13 (1980) 2609–2622.
[23] F. Nizzoli, J.R. Sandercock, in: G.K. Horton, A. Maradudin (Eds.), Dynamical Properties of Solids, Elsevier, New York, 1990.
[24] R. Loudon, Phys. Rev. Lett. 40 (1978) 581–583.
[25] A.M. Marvin, V. Bortolani, F. Nizzoli, J. Phys. C: Solid State Phys. 13 (1980) 299–317.
[26] G.W. Farnell, in: W.P. Mason, R.N. Thurston (Eds.), Physical Acoustics, vol. 6, Academic Press, New York, 1970, pp. 109–166.
[27] C. Sumanya, J.D. Comins, A.G. Every, J. Phys.: Conf. Ser. 92 (2007) 012103-1–012103-4.
[28] COMSOL Multiphysics finite element software.
[29] G.W. Farnell, E.L. Adler, in: W.P. Mason, R.N. Thurston (Eds.), Physical Acoustics, vol. 6, Academic Press, New York, 1972, pp. 35–127.
[30] N.G. Einspruch, L.T. Claiborne, J. Appl. Phys. 35 (1964) 175.
[31] J.R. Neighbours, G.A. Alers, Phys. Rev. 111 (1958) 707–712.
[32] H.J. McSkimin, J. Appl. Phys. 26 (1955) 406–409.
[33] A. Khelif, B. Aoubiza, S. Mohammadi, A. Adibi, V. Laude, Phys. Rev. E 74 (2006) 1–5.